

ORIGINAL RESEARCH

Phosphodiesterase 4 Inhibitor Roflupram Suppresses Inflammatory Responses Using Reducing Inflammasome in Microglia After Spinal Cord Injury

Piyun Sun, MD; Tianshu Zhao, MM; Jinlong Zhou, MM; Huiping Qi, MD; Guibin Qian, MD

ABSTRACT

Context • Neuroinflammation after spinal cord injury (SCI) can lead to long-term damage in neural tissue, which can cause the destruction and dysfunction of the neurological system. Roflupram (ROF), a selective phosphodiesterase 4 inhibitor, may play a protective role against neuropathological diseases, but the specific role of ROF in SCI treatment is unknown.

Objective • The study intended to investigate the anti-inflammatory mechanism and therapeutic effects of ROF to determine if it can attenuate lipopolysaccharide (LPS)-induced microglia that induces neuroinflammation and decrease neural-tissue damage following an SCI.

Design • The research team performed an animal study.

Setting • The study took place at the Fourth Affiliated Hospital of Harbin Medical University in Harbin, China.

Animals • The animals were female C57BL/6 mice, aged 8 weeks and weighing approximately 20 g.

Intervention • For the in-vitro study, the research team divided BV2 microglial cells into three groups: (1) the control group, which received no LPS stimuli and no ROF treatment, (2) the LPS group, which received LPS stimuli but no ROF treatment, and (3) LPS+ROF group, which received both LPS stimuli and ROF treatment. For the in-vivo study, the research team randomly divided the mice into three groups: (1) the sham group, for which the team didn't induce SCI and which received no ROF treatment (2) the SCI group, for which the team induced SCI but which received no ROF treatment, and (3) the SCI+ROF group, for which the team induced SCI and which received the ROF treatment.

Outcome Measures • The research team evaluated: (1) the cell viability of the BV2 microglia cells after five doses of ROF and the RNA levels of inflammatory-activation-related factors, the inflammatory pathway; (2) in-vitro inhibition of inflammation in LPS-activated microglia; (3) the anti-neuroinflammatory role of ROF after SCI induction in vitro; and (4) the role of ROF in neural-structure protection and locomotor-function recovery in vitro.

Results • In the in-vitro study, the ROF attenuated microglial inflammation through the inhibition of the NLRP3 inflammasome in vitro, reduced neuroinflammation, and protected against neuronal loss. In the in-vivo study with mice, the ROF: (1) improved the functional recovery of locomotor skills after induction of SCI; (2) acted in an anti-inflammatory role in SCI, restraining microglial inflammation by inhibition of the “nucleotide-binding domain, leucine-rich-containing family, pyrin domain-containing-3” (NLRP3) inflammasome and reduction of caspase-1-dependent, interleukin-1 beta (IL)-1 β ; and (3) reduced neuronal death and protected against tissue loss, improving functional recovery after an SCI.

Conclusions • The current study demonstrated that ROF can reduce the levels of inflammation in the tissue after spinal cord injury by modulating the AMPK/NLRP3 signaling pathway, thereby promoting the recovery of motor function in mice. ROF is a promising drug for prevention of neural-tissue damage following neural injury. (*Altern Ther Health Med.* 2023;29(7):340-347).

Piyun Sun, MD, Associate chief physician; **Jinlong Zhou, MM**, Associate chief physician; and **Huiping Qi, MD**, Associate chief physician; Department of Neurology, the Fourth Affiliated Hospital of Harbin Medical University, Harbin, China. **Tianshu Zhao, MM**, Associate chief physician, Department of Neurosurgery, the Fourth Affiliated Hospital of Harbin Medical University, Harbin, China. **Guibin Qian, MD**, Associate chief physician; Orthopedic Department, the

Fourth Affiliated Hospital of Harbin Medical University, Harbin, China.

Corresponding author: Guibin Qian, MD
E-mail: qgbqgb009@163.com

Spinal cord injury (SCI) is one of the most severe neurological diseases, resulting in paraplegia, bladder disorders, and even death in critical states.¹⁻³ Damaged neural tissue can provoke a series of pathophysiological events, such as neuroinflammation, oxidative stress, and apoptosis, that can aggravate an injury.^{4,5} Tran et al considers this process, named secondary SCI (SSCI), to be a crucial element affecting neurological recovery long-term.⁶

After an SCI, resident microglia become activated and work together with infiltrating leukocytes to release an increased amount of pro-inflammatory cytokines and reactive oxygen species (ROS). This induces neuroinflammation and can allow greater accumulation of glial groups and subsequent neural-tissue damage.^{7,8}

This inflammatory response can trigger processes such as demyelination, neuronal apoptosis, and pyroptosis. Excessive neurological damage can result in irreversible neurological dysfunction. Therefore, reducing neuroinflammation holds promise as a therapeutic approach to protect the integrity of neural tissue and preserve its function following an SCI.

Despite a few studies reporting that neuroinflammation can play a necessary part in effecting neurological repair,⁹ excessive activation of microglia following trauma can evoke larger and more serious neural-tissue loss in the injured area.

Phosphodiesterase 4 (PDE4)

PDE4 can catalyze cyclic adenosine monophosphate (cAMP) hydrolyzation,¹⁰ and inhibition of PDE4 can naturally provoke an increase in the cAMP level. Inhibition can increasingly initiate protein kinase A (PKA) and adenosine-monophosphate-activated protein kinase (AMPK),^{11,12} a critical metabolic enzyme that can induce suppression of the downstream “nucleotide-binding domain, leucine-rich-containing family, pyrin domain-containing-3” (NLRP3) inflammasome.

Previous studies have reported that a PDE4 inhibitor could induce phosphorylated expression of the AMPK-related pathway. For example, Wan et al reported that inhibition of phosphodiesterase could improve neuroprotection by activating AMPK for patients who had a stroke.¹³ Moreover, Zhong et al found that a PDE4 inhibitor could induce AMPK-dependent autophagy in an in-vitro Parkinson's model.¹⁴ Zhang et al found that activation of AMPK can suppress NLRP3 synthesis in inflammatory initiation.¹⁵ Ma et al found that AMPK phosphorylation could reduce NLRP3 expression in neurological diseases.¹⁶

NLRP3 Inflammasome

The NLRP3 inflammasome, which Tschopp first reported in 2002, is a notable pro-inflammatory protein complex that regulates the activation of caspase-1 and promotes interleukin-1 beta (IL-1 β) maturation.¹⁷ Several studies have shown that ROS can directly induce the synthesis of the NLRP3 complex, which is associated with the activation of toll-like receptor 4 (TLR4) and TNF receptors by LPS or TNF- α , respectively.¹⁸⁻²⁰

Macks et al mentioned the ameliorative effects of PDE4 inhibition in therapy for SCI and suggested the use of

Rolipram, the canonical PDE4 inhibitor, to promote neurite outgrowth and myelination in an SCI model.²¹ In addition, Schaal et al found that a PDE4 inhibitor could reduce inflammatory infiltration and oxidative stress in SCI.²²

Several other studies have demonstrated potent neuroprotection through inhibition of the NLRP3 inflammasome in several neurological diseases.²³⁻²⁵ Zhong et al found that inhibition of PDE4 could induce AMPK-dependent autophagy of neurons, after a “1-methyl-4-phenyl-1,2,3,6-tetrahydropyridine” (MPP)-induced oxidative insult.¹⁴

Roflupram (ROF)

Roflupram (ROF) is a selective PDE4 inhibitor and shows a high sensitivity against PDE4A4, PDE4B2 and PDE4D4.²⁶ More important, ROF can traverse the blood-brain barrier after oral administration and shows no side effects.

Recent studies have shown an ameliorative role for ROF in the neurological degeneration in Parkinson's disease (PD) and Alzheimer's disease (AD)²⁷⁻²⁸. You et al reported that ROF treatment can improve autophagy in microglial cells by inhibiting NLRP3 expression, leading to a subsequent reduction in caspase-1 and IL-1 β .²⁹

Current Study

The current research team has speculated that ROF treatment may play an anti-inflammatory and neuroprotective role in SCI and that the underlying mechanism may be inhibition of the inflammasome pathway in microglia.

The current study intended to investigate the anti-inflammatory mechanism and therapeutic effects of ROF to determine if it can attenuate lipopolysaccharide (LPS)-induced microglia that induces neuroinflammation and decrease neural-tissue damage following an SCI.

METHODS

Animals

The research team performed an animal study, which took place at the Fourth Affiliated Hospital of Harbin Medical University in Harbin, China. The animals were female C57BL/6 mice, aged 8 weeks and weighing approximately 20 g. The research team obtained them from and housed them at the university's Animal Center. All experimental animals were provided ad libitum access to food and water throughout the experiment. They were housed in an animal facility with a controlled environment of 50% relative humidity, a temperature of 22 \pm 1 degrees Celsius, and a 12/12 light-dark cycle. The center's Animal Ethics Committee approved the study's protocols.

Procedures

Materials and equipment. The research team purchased: (1) from American Type Culture Collection (ATCC, Virginia, USA), the BV2 microglia cell line; (2) from Gibco (Rockville, MD, USA), Dulbecco's Modified Eagle Medium (DMEM), fetal bovine serum (FBS), and 1% penicillin/streptomycin; (3) from Sigma-Aldrich (St. Louis, MO, USA), ROF, 0.1%

dimethylsulfoxide (DMSO), and lipopolysaccharide (LPS); (4) from Beyotime (Shanghai, China), a Cell Counting Kit 8 (CCK8) solution, a Total Protein Extraction Kit, a Bicinchoninic Acid (BCA) Assay Kit, and an HE Staining Kit; (5) from BioTek Instruments Inc., (Winooski, VT, USA), a microplate reader; (6) from Sigma-Aldrich (St. Louis, MO, USA), 1% pentobarbital sodium; (7) from Invitrogen (Carlsbad, CA, USA), a TRIzol Plus RNA Purification Kit and the SuperScript IV One-Step Reverse transcription-polymerase chain reaction (RT-PCR) system; (8) from Thermo Scientific (Waltham, MA, USA), a Maxima H Minus First Strand cDNA Synthesis Kit; (9) from Beyotime (Shanghai, China), 4% paraformaldehyde (PFA); (10) from Leica (Wetzlar, Germany) (Shanghai, China), a rotary microtome; (11) from Abcam (Cambridge, MA, USA), ionized calcium-binding adapter molecule 1 (IBA-1), cluster of differentiation 86 (CD86), hypophosphorylated neurofilament H (NF200), NLRP3, IL-1 β , caspase-1, Alexa Fluor 488 and 594, diamidine phenylindole (DAPI) Mounting Medium With DAPI-Aqueous Fluoroshield, p-AMPK, AMPK, glyceraldehyde 3-phosphate dehydrogenase (GAPDH), and goat anti-rabbit IgG H&L (HRP); (12) from Leica (Wetzlar, Germany), a fluorescence inversion microscope system (DMI600 B FW4000); (13) from R&D Systems (Minneapolis, MN, USA), an enzyme-linked immunosorbent assay (ELISA), (14) from BioRed (Hercules, CA, USA), an enhanced chemiluminescence (ECL) system, and (15) from Beyotime (Shanghai, China), the 3,3', 5,5'-tetramethylbenzidine (TMB) solution.

In-vitro groups. For the evaluation of the effects of ROF on microglial cells in vitro, the research team divided the cells into three groups: (1) the control group, which received no LPS stimuli and no ROF treatment, (2) the LPS group, which received LPS stimuli but no ROF treatment, and (3) LPS+ROF group, which received both LPS stimuli and ROF treatment.

Cell culture and treatment. The research team: (1) cultured the BV2 microglial cells in six-well plates containing 4 mL of DMEM; (2) supplemented the medium with 10% FBS and 1% penicillin/streptomycin; (3) for cell treatment, dissolved five concentrations of ROF—5 μ M, 10 μ M, 20 μ M, 50 μ M, and 100 μ M—in DMEM with DMSO and added the cell medium for 24h; and (4) dissolved 1 μ g/mL of LPS in DMEM and added it to the treated cells for 16 h.

Cell viability assay. The research team: (1) cultured the BV2 microglial cells—1x10⁴ /well—in 96-well plates overnight at 37°C and 5% CO₂; (2) removed the culture medium with the 5 μ M to 100 μ M amounts of ROF and added the medium into separate wells; (3) incubated the cells for 2 h; (4) measured cell viability using the CCK8, following the manufacturer's instructions; and (5) measured absorbance using the microplate reader at 450 nm.

In-vivo groups. For the in-vivo study, the research team randomly divided the mice into three groups and applied distinct labeling to differentiate them in each group: (1) the sham group, for which the team didn't induce SCI and which received no ROF treatment (2) the SCI group, for which the team induced SCI but which received no ROF treatment, and

Table 1. Primer Sequences of Quantitative Reverse Transcription-Polymerase Chain Reaction

Oligo Name		Sequence (5' -----> 3')
NF- κ B	Forward	AGAGGGGATTTTCGATTCCGC
	Reverse	CCTGTGGGTAGGATTTCTTGTC
COX-2	Forward	TGCACTATGGTTACAAAAGCTGG
	Reverse	TCAGGAAGCTCCTTATTTCCCTT
iNOS	Forward	GTTCTCAGCCCAACAATACAAGA
	Reverse	GTGGACGGTTCGATGTCAC
GAPDH	Forward	AGGTCGGTGTGAACGGATTTG
	Reverse	TGTAGACCATGTAGTTGAGGTCA

Abbreviations: COX-2, cyclooxygenase-2; GAPDH, glyceraldehyde 3-phosphate dehydrogenase; iNOS, inducible nitric oxide synthase; NF- κ B, nuclear factor kappa-light-chain-enhancer of activated B cells

(3) the SCI+ROF group, for which the team induced SCI and which received the ROF treatment.

SCI induction. The surgical procedure for SCI was the same as that performed in the current research team's previous study.³⁰ Briefly, for the SCI and SCI+ROF groups, the team: (1) anesthetized the mice intraperitoneally, using 50 mg/kg of 1% pentobarbital sodium and (2) exposed and compressed the 10th thoracic spinal cord using 50 kilodyne for 2 min. Following the SCI+ROF group's recovery, the team administered 10 mg/kg qd of ROF, dissolved in normal saline, using oral gavage for a week after the SCI.

RT-PCR. The research team: (1) extracted total RNA from the BV2 cells or the animals' cord tissues using the TRIzol Plus RNA Purification Kit, following the manufacturer's protocols; (2) conducted complementary deoxyribose nucleic acid (cDNA) synthesis using the RT-PCR system; (3) employed a melting curve to analyze each RNA level; (4) applied glyceraldehyde 3-phosphate dehydrogenase (GAPDH) for normalization; and (5) quantified relative levels of mRNA expression using the 2- $\Delta\Delta$ Ct methods. Table 1 shows the formulated mentioned primers of RNAs.

IF staining. The research team: (1) fixated the spinal cord tissue with the 4% PFA for 24 h and conducted dehydration through different gradients of alcohol; (2) embedded the samples into paraffin; and (3) cut them into 5- μ m sections using the rotary microtome.

For IF, the team: (1) incubated sections overnight at 4°C with IBA-1 at 1:300, CD86 at 1:200, NF200 at 1:200, NLRP3 at 1:200, IL-1 β at 1:100, and caspase-1 at 1:100; (2) washed the sections and incubated them with Alexa Fluor 488 or 594 at 1:200 for one hour; (3) stained the nuclei with the DAPI mounting medium; and (4) visualized and collected the images of sections using the fluorescence inversion microscope system.

HE staining. For histologic observation, the research team conducted HE staining according to the manufacturer's protocols; (2) counterstained the nuclei with hematoxylin for 10 s; and (3) observed the images using a fluorescence inversion microscope system.

Western blotting. The research team: (1) for the microglia, performed lysis using the total protein extraction kit, according

to the manufacturer's protocols; (2) quantified the data using the BCA assay kit; (3) determined equivalent protein by carrying out 10% sodium dodecyl sulfate polyacrylamide gel electrophoresis (SDS-PAGE) for approximately 90 min; and (4) continued the transfer and immuno-blocking.

The team subsequently incubated the primary and secondary antibodies. The antibodies in the Western blot were: p-AMPK at 1:1000, AMPK at 1:1000, NLRP3 at 1:1000, caspase-1 at 1:1000, GAPDH at 1:2000, and HRP at 1:2000. The team used the ECL system to show the protein.

ELISA. The research team measured proinflammatory cytokines using ELISA. Briefly, the team: (1) added the samples into 96-well plates; (2) incubated the ELISA reactive reagents with samples in sequence, according to the manufacturer's instructions; and (3) after adding the TMB solution and treating the samples for 20 min in the dark, terminated the reaction and detected the cytokines at 450 nm using a microplate reader.

Basso Mouse Scale (BMS).³¹ Mice in each group were allowed free movement in an open field for 4 min on days 1, 3, 7, 14, 21, and 28 days after the SCI induction (dpi). Two researchers, who were blinded to the group allocation, assessed the motor function of the experimental mice using the BMS scoring system. The assessors were trained prior to the scoring to ensure their proficiency in using the BMS scoring criteria. The team then collected the data using Microsoft Excel (Microsoft, Redmond, WA, USA) and statistically analyzed it.

Outcome measures. The research team evaluated: (1) the cell viability of the BV2 microglia cells after five doses of ROF and the RNA levels of inflammatory-activation-related factors, the inflammatory pathway; (2) in-vitro inhibition of inflammation in LPS-activated microglia; (3) the anti-neuroinflammatory role of ROF after SCI induction in vitro; and (4) the role of ROF in neural-structure protection and locomotor-function recovery in vitro.

Outcome Measures

LPS-induced microglial activation. The research team investigated whether ROF can affect the cell viability of the BV2 microglia cells. The team examined the cell viability for the five doses of ROF, 5 μ M to 100 μ M, using the CCK8 assay. The team also measured the RNA levels of inflammatory, activation-related factors, including inducible nitric oxide synthase (iNOS), cyclooxygenase-2 (COX-2), and nuclear factor kappa-light-chain-enhancer of activated B cells (NF- κ B), using RT-PCR.

Inflammation. A previous study has shown that ROF exerts neuroprotective effects by activating AMPK.²⁹ The research team therefore explored whether ROF can inhibit inflammation in LPS-activated microglia using regulation of AMPK and downstream NLRP3.

Neuroinflammation after SCI induction. In vivo, the research team further evaluated the anti-neuroinflammatory role of ROF after SCI induction by extracted fresh spinal cords at 3 dpi for RNA detection. The team also measured: (1) the levels of NLRP3 and caspase-1 using IF staining and (2) pro-inflammatory cytokines using ELISA.

Tissue loss and functional recovery. The research team investigated the role of ROF in neural-structure protection and locomotor-function recovery, using IF staining to verify the number of neurofilaments at 28 dpi. In addition, the team: (1) assessed the ROF treatment's benefits for tissue protection using HE staining and (2) evaluated the locomotor-function recovery at 1, 3, 7, 14, 21, and 28 dpi, using the BMS.

Statistical Analysis

The research team collected and analyzed the data using Statistical Product and Service Solutions (SPSS) 21.0 software (IBM, Armonk, NY, USA). The team (1) expressed measurement data as means \pm standard deviations (SDs) and compared differences between two groups using the Student's *t* test and among more than two groups using an analysis of variance (ANOVA). *P* < .05 indicated statistical significance.

RESULTS

LPS-induced Microglial Activation

No significant difference existed in cell viability between any dose of ROF and the control group (Figure 1A). The research team selected the optimum concentration, 20 μ M of ROF, to investigate its effects against iNOS, COX-2, and NF- κ B.

After the LPS treatment, the RNA levels of iNOS, COX-2, and NF- κ B in the LPS and LPS+ROF groups were significantly higher than those of the control group, but the LPS+ROF group's levels were significantly lower than those of the LPS group (Figures 1B-1D).

Moreover, the IF staining showed that CD86-positive microglia increased in the LPS group. However, the ROF significantly inhibited the number of CD86-positive activated microglia after LPS stimuli (Figure 1E), indicating that ROF can significantly alleviate inflammatory microglia activation following LPS employment.

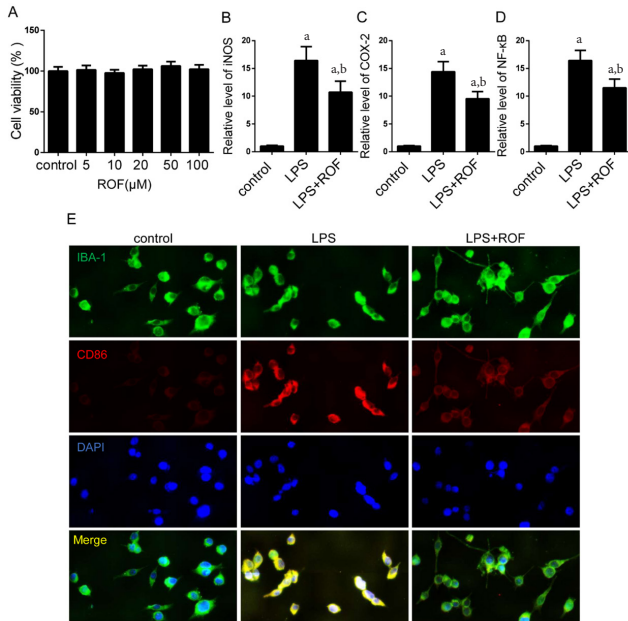
Cell Inflammation

Western blotting showed that the expressions of p-AMPK and NLRP3 in the LPS and LPS+ROF groups were significantly higher than those of the control group. However, the LPS+ROF group's p-AMPK level was significantly higher and its NLRP3 level was significantly lower than those of the LPS group (Figure 2A-2C).

Moreover, IF staining for caspase-1 and IL-1 β showed that the ROF treatment in activated microglia could reduce the expressions of caspase-1 and IL-1 β , which were highly expressed after NLRP3 accumulation (Figure 2D). This indicates that ROF administration could reverse an LPS-induced inflammatory response in BV2 microglia.

The ELISA showed that the expressions of TNF- α and IL-6 in the LPS and LPS+ROF groups were significantly higher than those of the control group. However, the LPS+ROF group's levels of TNF- α and IL-6 in inflammatory-activated microglia were significantly lower than those of the LPS group (Figure 2E and 2F). The results demonstrate that ROF can mitigate inflammation using activation of AMPK and reduction of the NLRP3/ caspase-1/ IL-1 β axis.

Figure 1. ROF's Attenuation of LPS-induced Microglial Activation in the Control, LPS, and LPS+ROF Groups. Figure 1A shows the representative cell viability of BV2 microglia when treated with 5 μ M to 100 μ M of ROF. Figures 1B-1D show the representative RNA expressions of iNOS, COX-2, and NF- κ B. Figure 1E shows the representative IF staining of IBA-1 (Green) and CD86 (Red), with a 400X magnification.



^a $P < .05$, indicating that the LPs group's and the LPS+ROF group's iNOS, COX-2, and NF- κ B levels were significantly higher than those of the control group
^b $P < .05$, indicating that the LPS+ROF group's iNOS, COX-2, and NF- κ B levels were significantly lower than those of the LPS group

Abbreviations: CD86, cluster of differentiation 86; COX-2, cyclooxygenase-2; IBA-1, ionized calcium-binding adapter molecule 1; iNOS, inducible nitric oxide synthase; LPS, lipopolysaccharide; NF- κ B, nuclear factor kappa-light-chain-enhancer of activated B cells; ROF, Roflupram.

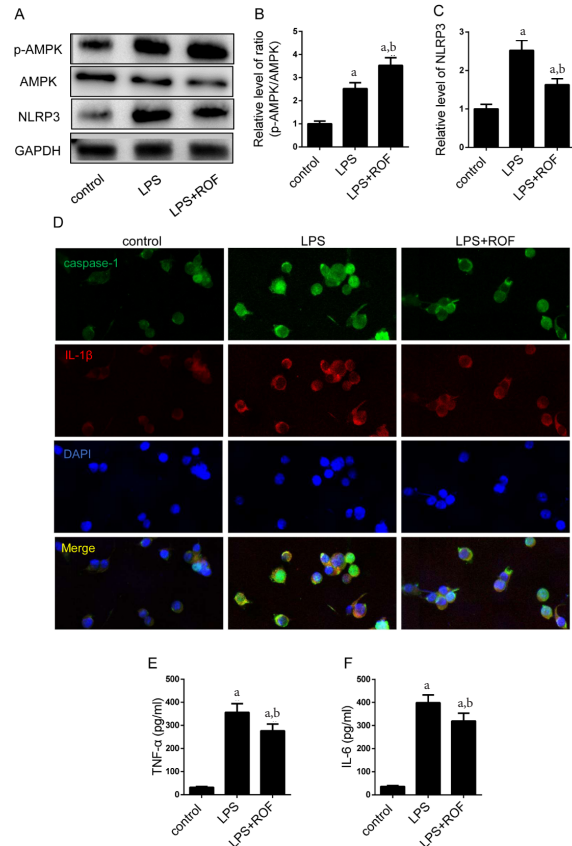
Neuroinflammation After SCI Induction

The RT-PCR showed that the RNA expressions of iNOS, COX-2, and NF- κ B were significantly higher in the SCI and SCI+ROF groups at the injured sites after SCI induction than those of the sham group. However, the SCI+ROF group's levels were significantly lower than those of the SCI group (Figure 3A-3C).

The IF staining showed that the levels of NLRP3 and caspase-1 significantly increased expression of NLRP3 and caspase-1 after SCI induction. However, mice treated with ROF showed a decrease in NLRP3 and caspase-1 at the injury sites at 3 dpi compared with the SCI group (Figure 3D).

Moreover, the levels of TNF- α , IL-1 β , and IL-6 for the SCI and SCI+ROF groups at the injury sites at 3 dpi were significantly higher than those of the sham group, SCI+ROF

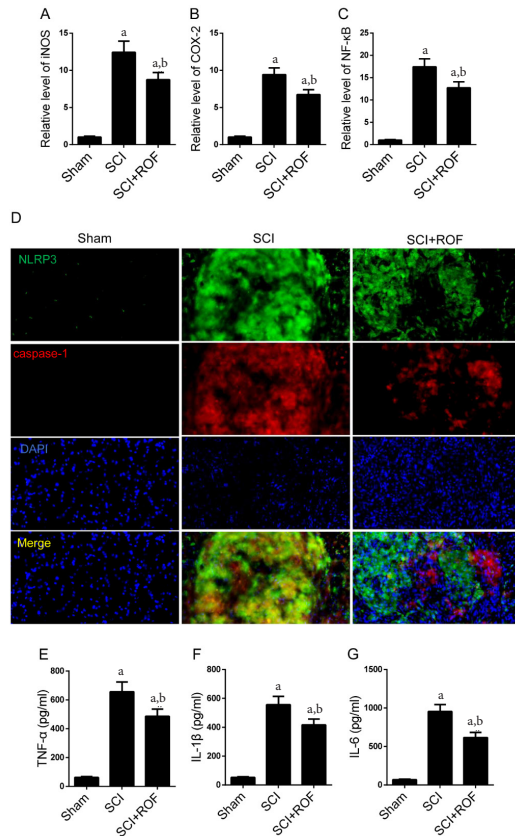
Figure 2. ROF's Mitigation of Inflammation in the Control, LPS, and LPS+ROF Groups Through Activation of the AMPK/ NLRP3/Caspase-1 Axis in Microglia. Figure 2A shows the representative Western blotting of p-AMPK, AMPK, and NLRP3. Figures 2B and 2C show the quantitation of p-AMPK/AMPK and NLRP3. Figure 2D shows the representative IF staining of caspase-1 (Green) and IL-1 β (Red), with a 400X magnification. Figures 2 E and 2F show the representative ELISA of TNF- α and IL-6.



^a $P < .05$, indicating that the LPs group's and the LPS+ROF group's pAMPK, NLRP3, TNF- α , and IL-6 levels were significantly higher than those of the control group
^b $P < .05$, indicating that the LPS+ROF group's pAMPK level was significantly higher and it levels of NLRP3, TNF- α , and IL-6 levels were significantly lower than those of the LPS group

Abbreviations: AMPK, adenosine monophosphate (AMP)-activated protein kinase; ELISA, enzyme-linked immunosorbent assay; IF, immunofluorescence; IL-1 β , interleukin-1 beta; IL-6, interleukin-6; LPS, lipopolysaccharide; NLRP3, nucleotide-binding domain, leucine-rich-containing family, pyrin domain-containing-3; ROF, Roflupram; TNF- α , tumor necrosis factor alpha.

Figure 3. ROF's Reduction of Neuroinflammation in the Sham, SCI and SCI+ROF Groups After SCI. Figures 3A-3C show the representative RNA levels of iNOS, COX-2, and NF-κB at 3 dpi. Figure 3D shows the representative IF staining of NLRP3 (Green) and caspase-1 (Red) at 3 dpi, with a 400× magnification. Figures 3E-3G show the representative ELISA of TNF-α, IL-1β and IL-6 at 3 dpi.

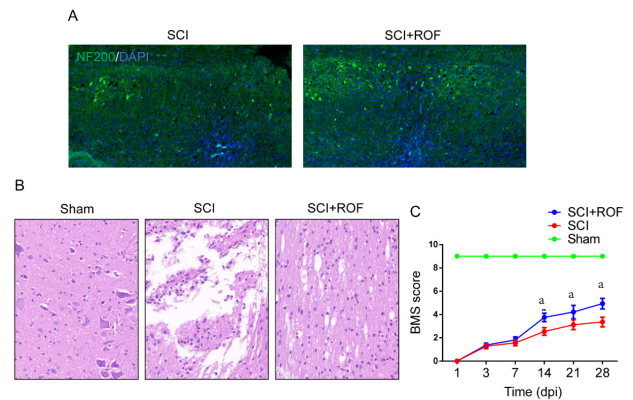


^a $P < .05$, indicating that the SCI group's and the SCI+ROF group's iNOS, COX-2, NF-κB, TNF-α, IL-1β, and IL-6 levels were significantly higher than those of the sham group

^b $P < .05$, indicating that the SCI+ROF group's iNOS, COX-2, NF-κB, TNF-α, IL-1β, and IL-6 levels were significantly lower than those of the SCI group

Abbreviations: dpi, days post SCI induction; COX-2, cyclooxygenase-2; ELISA, enzyme-linked immunosorbent assay; IL-1β, interleukin-1 beta; IL-6, interleukin-6; iNOS, inducible nitric oxide synthase; NF-κB, nuclear factor kappa-light-chain-enhancer of activated B cells; NLRP3, nucleotide-binding domain, leucine-rich-containing family, pyrin domain-containing-3; ROF, Roflupram; SCI, spinal cord injury; TNF-α, tumor necrosis factor alpha.

Figure 4. ROF's Protection Against Tissue Loss and Promotion of Functional Recovery in the Sham, SCI, and SCI+ROF groups. Figure 4A shows the representative IF staining of NF200 at 28 dpi, with 100× magnification. Figure 4B shows the representative HE staining at 28 dpi, with a 200X magnification. Figure 4C shows the representative BMS scores at 1, 3, 7, 14, 21, and 28 dpi.



^a $P < .05$, indicating that the SCI+ROF group's BMS scores were significantly higher than those of the SCI group at days 14, 21, and 28

Abbreviations: BMS, Basso Mouse Scale; HE, hematoxylin and eosin; IF, immunofluorescence; ROF, Roflupram; SCI, spinal cord injury.

group's levels in the injured spinal cords were significantly lower than those of the SCI group (Figure 3E-3G). These results indicate that treatment with ROF can reduce neuroinflammation using inhibition of the NLRP3/ caspase-1 axis after SCI.

Tissue Loss and Functional Recovery

At 28 dpi, the SCI+ROF group had more NF200-positive neurofilaments at injured sites compared with the SCI group (Figure 4A). The SCI+ROF had a much lower level of tissue incompleteness at 28 dpi compared with the SCI group (Figure 4B). The SCI+ROF group's mean BMS scores for locomotor function beginning at 14 dpi were significantly higher than those of the SCI group (Figure 4C). Therefore, the results suggest that ROF use can ameliorate neural-tissue loss and improve locomotor-function recovery after SCI.

DISCUSSION

The current study found that ROF treatment can inhibit neuroinflammation and protect neural tissue after SCI induction by specifically inhibiting the NLRP3/caspase-1/ IL-1β axis. Therefore, ROF is a promising reagent to attenuate neuroinflammation following trauma.

One of the current study's major findings is that ROF, as a selective PDE4 inhibitor, can reduce microglia-induced neuroinflammation using regulation of the AMPK/ NLRP3 axis. Additionally, the study found that administration of

ROF can lead to a decrease in the expressions of downstream caspase-1 and IL-1 β .

The current study also demonstrated that ROF can play an important role in inhibiting the LPS-induced NLRP3 synthesis in BV2 cells. Regarding ROF's actions as a selective PDE4 inhibitor, no researchers have reported an anti-neuroinflammatory role for it in SCI yet. Considering that previous studies have shown ROF's suppression of inflammasome activation in various diseases,³²⁻³³ the current research team was intrigued to investigate the potential of ROF in exerting a negative effect on neuroinflammatory events following spinal cord injury (SCI).

In the current study, the research team consistently observed that administration of ROF in LPS-induced BV2 microglial cells could decrease expressions of NLRP3, caspase-1, and IL-1 β . Furthermore, the team verified that ROF could inhibit changes in NLRP3 levels by upregulating AMPK phosphorylation. Additionally, the team found that ROF treatment can reduce NF- κ B levels in microglia. Consequently, the current study found that the increased expressions of iNOS and COX-2 were reversed following ROF treatment. The overall effects of ROF were a decreased activation of microglia.

The current research team's discovery that ROF can alleviate neuroinflammation provides a promising avenue for safeguarding neural tissue after SCI. Consistently, the current study's HE staining showed a reduced area of damage in the injured spinal cord of the SCI+ROF group compared to the SCI group.

Additionally, when examining the structure of neurofilaments surrounding the injury site, the current study found that the SCI+ROF group exhibited a more-intact neurofilament architecture compared to the SCI group. These findings indicate that the administration of ROF can effectively prevent secondary injury to the spinal-cord tissue. The research team noticed an ameliorative motor-function recovery in the SCI+ROF group.

The current study investigated the potential of ROF in modulating the AMPK pathway, which is involved in regulating cellular bioenergy metabolism and plays a central role in various diseases. The research team found that treatment with ROF can induce an increase in AMPK phosphorylation levels in an in-vitro microglial inflammation model. The current research team observed similar results in the in-vivo mouse model.

The decline of inflammasome NLRP3 in the current study resulted in inhibition of the expression of pro-inflammatory factors such as IL-1 β , TNF- α , and IL-6, and thereby, the levels of inflammation decreased after SCI. Therefore, the current research team suggests that ROF can have anti-inflammatory properties in an SCI model.

The current study had some limitations. The research team discovered that ROF can alleviate inflammation through AMPK/ NLRP3 signaling pathway in microglia but failed to exclude the possibility of other synergetic or independent relative pathways in neuroinflammation response. Moreover,

in this study, we did not use an AMPK-specific inhibitor to reverse the effect of ROF, further confirming the specific mechanism by which ROF inhibits inflammasome activation. Indispensably, ROF was also found to induce autophagy in neurologic disorders. ROF exerts need to devote more research to autophagy regulation in the future.

CONCLUSIONS

The current study demonstrated that ROF can reduce the levels of inflammation in the tissue after spinal cord injury by modulating the AMPK/NLRP3 signaling pathway, thereby promoting the recovery of motor function in mice. Therefore, ROF is a promising drug for prevention of neural-tissue damage following neural injury.

AUTHORS' DISCLOSURE STATEMENT

The Scientific and Technological Innovation Talents Project of the Fourth Affiliated Hospital of Harbin Medical University (HYDSYCXRC202149) supported the study. The authors declare that they have no conflicts of interest related to the study.

REFERENCES

- Ahuja CS, Wilson JR, Nori S, et al. Traumatic spinal cord injury. *Nat Rev Dis Primers*. 2017;3(1):17018. doi:10.1038/nrdp.2017.18
- Kaplan SA, Chancellor MB, Blaiwas JG. Bladder and sphincter behavior in patients with spinal cord lesions. *J Urol*. 1991;146(1):113-117. doi:10.1016/S0022-5347(17)37727-3
- Azarhomayoun A, Aghasi M, Mousavi N, et al. Mortality Rate and Predicting Factors of Traumatic Thoracolumbar Spinal Cord Injury: A Systematic Review and Meta-Analysis. *Bull Emerg Trauma*. 2018;6(3):181-194. doi:10.29252/beat-060301
- Saxena T, Loomis KH, Pai SB, et al. Nanocarrier-mediated inhibition of macrophage migration inhibitory factor attenuates secondary injury after spinal cord injury. *ACS Nano*. 2015;9(2):1492-1505. doi:10.1021/nn505980z
- Wang Z, Nong J, Shultz RB, et al. Local delivery of minocycline from metal ion-assisted self-assembled complexes promotes neuroprotection and functional recovery after spinal cord injury. *Biomaterials*. 2017;112:62-71. doi:10.1016/j.biomaterials.2016.10.002
- Tran AP, Warren PM, Silver J. The Biology of Regeneration Failure and Success After Spinal Cord Injury. *Physiol Rev*. 2018;98(2):881-917. doi:10.1152/physrev.00017.2017
- Papa S, Caron I, Erba E, et al. Early modulation of pro-inflammatory microglia by minocycline loaded nanoparticles confers long lasting protection after spinal cord injury. *Biomaterials*. 2016;75:13-24. doi:10.1016/j.biomaterials.2015.10.015
- Zhou X, Wahane S, Friedl MS, et al. Microglia and macrophages promote coralling, wound compaction and recovery after spinal cord injury via Plexin-B2. *Nat Neurosci*. 2020;23(3):337-350. doi:10.1038/s41593-020-0597-7
- Candelario-Jalil E, Dijkhuizen RM, Magnus T. Neuroinflammation, Stroke, Blood-Brain Barrier Dysfunction, and Imaging Modalities. *Stroke*. 2022;53(5):1473-1486. doi:10.1161/STROKEAHA.122.036946
- Wu C, Rajagopalan S. Phosphodiesterase-4 inhibition as a therapeutic strategy for metabolic disorders. *Obes Rev*. 2016;17(5):429-441. doi:10.1111/obr.12385
- Wang Z, Liang Y, Zhang L, Zhang N, Liu Q, Wang Z. Phosphodiesterase 4 inhibitor activates AMPK-SIRT6 pathway to prevent aging-related adipose deposition induced by metabolic disorder. *Aging (Albany NY)*. 2018;10(9):2394-2406. doi:10.18632/aging.101559
- Kim DU, Kwak B, Kim SW. Phosphodiesterase 4B is an effective therapeutic target in colorectal cancer. *Biochem Biophys Res Commun*. 2019;508(3):825-831. doi:10.1016/j.bbrc.2018.12.004
- Wan D, Zhou Y, Wang K, Hou Y, Hou R, Ye X. Resveratrol provides neuroprotection by inhibiting phosphodiesterases and regulating the cAMP/AMPK/SIRT1 pathway after stroke in rats. *Brain Res Bull*. 2016;121:255-262. doi:10.1016/j.brainresbull.2016.02.011
- Zhong J, Xie J, Xiao J, et al. Inhibition of PDE4 by FCPR16 induces AMPK-dependent autophagy and confers neuroprotection in SH-SY5Y cells and neurons exposed to MPP (+)-induced oxidative insult. *Free Radical Bio Med*. 2019;135(87-101). doi:10.1016/j.freeradbiomed.2019.02.027
- Zhang H, Gong X, Ni S, Wang Y, Zhu L, Ji N. C1q/TNF-related protein-9 attenuates atherosclerosis through AMPK-NLRP3 inflammasome signaling pathway. *Int Immunopharmacol*. 2019;77:105934. doi:10.1016/j.intimp.2019.105934
- Ma C, Wang X, Xu T, et al. Qingkailing injection ameliorates cerebral ischemia-reperfusion injury and modulates the AMPK/NLRP3 Inflammasome Signaling pathway. *BMC Complement Altern Med*. 2019;19(1):320. doi:10.1186/s12906-019-2703-5
- Martinon F, Burns K, Tschopp J. The inflammasome: a molecular platform triggering activation of inflammatory caspases and processing of proIL-beta. *Mol Cell*. 2002;10(2):417-426. doi:10.1016/S1097-2765(02)00599-3
- Lebreton F, Berishvili E, Parnaud G, et al. NLRP3 inflammasome is expressed and regulated in human islets. *Cell Death Dis*. 2018;9(7):726. doi:10.1038/s41419-018-0764-x
- Liu H, Xiong J, He T, et al. High Uric Acid-Induced Epithelial-Mesenchymal Transition of Renal Tubular Epithelial Cells via the TLR4/NF- κ B Signaling Pathway. *Am J Nephrol*. 2017;46(4):333-342. doi:10.1159/000481668
- Zhang Y, Yang X, Qiu C, Liu F, Liu P, Liu Z. Matrine suppresses AGE-induced HAEC injury by inhibiting ROS-mediated NLRP3 inflammasome activation. *Eur J Pharmacol*. 2018;822:207-211. doi:10.1016/j.ejphar.2018.01.029
- Macks C, Gwak SJ, Lynn M, Lee JS. Rolipram-Loaded Polymeric Micelle Nanoparticle Reduces Secondary Injury after Rat Compression Spinal Cord Injury. *J Neurotrauma*. 2018;35(3):582-592. doi:10.1089/neu.2017.5092
- Schaal SM, Garg MS, Ghosh M, et al. The therapeutic profile of rolipram, PDE target and mechanism of action as a neuroprotectant following spinal cord injury. *PLoS One*. 2012;7(9):e43634. doi:10.1371/journal.pone.0043634
- Feng J, Wang JX, Du YH, et al. Dihydropyridinone inhibits microglial activation and neuroinflammation by suppressing NLRP3 inflammasome activation in APP/PS1 transgenic mice. *CNS Neurosci Ther*. 2018;24(12):1207-1218. doi:10.1111/cns.12983

24. Xu X, Yin D, Ren H, et al. Selective NLRP3 inflammasome inhibitor reduces neuroinflammation and improves long-term neurological outcomes in a murine model of traumatic brain injury. *Neurobiol Dis*. 2018;117:15-27. doi:10.1016/j.nbd.2018.05.016
25. Yap JKY, Pickard BS, Chan EWL, Gan SY. The Role of Neuronal NLRP1 Inflammasome in Alzheimer's Disease: Bringing Neurons into the Neuroinflammation Game. *Mol Neurobiol*. 2019;56(11):7741-7753. doi:10.1007/s12035-019-1638-7
26. Zhong J, Dong W, Qin Y, et al. Roflupram exerts neuroprotection via activation of CREB/PGC-1 α signalling in experimental models of Parkinson's disease. *Br J Pharmacol*. 2020;177(10):2333-2350. doi:10.1111/bph.14983
27. Dong WL, Zhong JH, Chen YQ, et al. Roflupram protects against rotenone-induced neurotoxicity and facilitates α -synuclein degradation in Parkinson's disease models. *Acta Pharmacol Sin*. 2021;42(12):1991-2003. doi:10.1038/s41401-021-00768-4
28. Wang X, Zhang R, Lin Y, Shi P. Inhibition of NF- κ B might enhance the protective role of roflupram on SH-SY5Y cells under amyloid β stimulation via PI3K/AKT/mTOR signaling pathway. *Int J Neurosci*. 2021;131(9):864-874. doi:10.1080/00207454.2020.1759588
29. Li D, Xu J, Qin Y, Cai N, Cheng Y, Wang H; Roflupram, a novel phosphodiesterase 4 inhibitor, inhibits lipopolysaccharide-induced neuroinflammatory responses through activation of the AMPK/Sirt1 pathway. *Int Immunopharmacol*. 2021;90(107176). doi:10.1016/j.intimp.2020.107176
30. Sun P, Zhou J, Zhao T, Qi H, Qian G. Zileuton Ameliorates Neuronal Ferroptosis and Functional Recovery After Spinal Cord Injury. *Altern Ther Health Med*. 2023 Jul;29(5):314-319. PMID: 37171943.
31. Jin Z, Tian L, Zhang Y, et al. Apigenin inhibits fibrous scar formation after acute spinal cord injury through TGF β /SMADs signaling pathway. *CNS Neurosci Ther*. 2022;28(11):1883-1894. doi:10.1111/cns.13929
32. Xie J, Bi B, Qin Y, et al; Inhibition of phosphodiesterase-4 suppresses HMGB1/RAGE signaling pathway and NLRP3 inflammasome activation in mice exposed to chronic unpredictable mild stress. *Brain Behav Immun*. 2021;92(67-77). doi:10.1016/j.bbi.2020.11.029
33. Zhou Q, Zhang Y, Lu L, et al; Upregulation of postsynaptic cAMP/PKA/CREB signaling alleviates copper(II)-induced oxidative stress and pyroptosis in MN9D cells. *Toxicology*. 2023;494(153582). doi:10.1016/j.tox.2023.153582